07,10

Thermodynamic stability and pathways for the formation of core-shell states in stratified systems of small volume

© V.B. Fedoseev

Razuvaev Institute of Organometallic Chemistry, Russian Academy of Sciences,
Nizhny Novgorod, Russia

E-mail: vbfedoseev@yandex.ru

Received October 3, 2024
Revised October 4, 2024
Accepted October 5, 2024

Size effects during phase transitions in a binary stratified mixture in a small volume are simulated using chemical thermodynamics methods. The results are describing the conditions for the existence of stable, metastable and unstable thermodynamically equilibrium states using the example of a Bi–Sb solid solution. An energy surface has been created that displays all states of a stratified solution in a system with a core-shell structure. Energy profiles for optimal pathways between homogeneous and heterogeneous equilibrium states are shown. Critical nucleus states are identified. As the volume of the stratifying solution decreases, the homogeneous state becomes metastable and its stability increases. At the same time, heterogeneous states lose stability, become metastable and disappeared. The composition of the mixture also affects the energies of formation and stability of heterogeneous states.

Keywords: phase transformations, size effect, stratifying solutions, metastable states, critical nucleus.

DOI: 10.61011/PSS.2024.11.60103.252

1. Introduction

The peculiarities of chemical and phase transformations in a small volume have become the basis for the emergence of new effective chemical technologies that make it possible to obtain materials with unusual properties, composition and morphology. The multiple increase of the speed of physical and chemical processes in a small volume and the possibility of chemical reactions that are not realized in macroscopic systems are of great interest for the technology [1,2]. The combined flow of chemical and phase transformations can significantly affect the kinetics of chemical reactions in a small volume and the properties of the system [3]. We have described similar effects by methods of chemical thermodynamics and reproduced experimentally using the example of the polycondensation reaction in a spray [4–6].

Micro- and nanostructured materials are used in many areas of the economy, so their stability is one of the key properties. The thermodynamic stability of such materials with phase transformations is important for the creation and use of catalysts [7,8], pharmaceutical drugs [9,10], development of promising methods of energy storage and conversion [11–13] and other applications [14]. This makes relevant the thermodynamic analysis of the size effects accompanying the formation of new phases and the stability of emerging structures [15].

The purpose of this paper is to evaluate the energy effects of phase transformations and the stability of the states that occur during such transformations. Methods of chemical thermodynamics based on Gibbs energy analysis and the construction of diagrams showing the thermodynamic stability of stable and metastable states for small volume systems are used for this [16,17].

2. Thermodynamic description of a demixing solution in a small volume system

The term thermodynamic stability of states is defined in the usual way — it is a spontaneous return to the considered state with small changes in thermodynamic parameters. The states corresponding to the energy minima of the system possess this property. The concepts of stable and metastable states denote global and local energy minima.

The features of phase transformations in small volume systems are associated with an increase of the contribution of the energy of the interphase boundaries to the total energy of the system. This contribution becomes significant for micro- and nano-objects and manifests itself in the form of size effects. These effects manifest themselves in phase diagrams as a shift of critical points and a region of heterogeneity [8,18,19].

Chemical thermodynamics describes the general laws of phase transformations in systems of limited size. The thermodynamic description is based on the calculation and minimization of the Gibbs energy (G) of the mixture and is implemented in CALPHAD (CALculation of PHAse Diagrams) or nano-CALPHAD methods [20–22] and in the statistical thermodynamics methods [23]. The size effects for clusters are reproduced by molecular dynamics methods [24–26], which also allow evaluating the stability of formed structures [27].

Our approach complements the CALPHAD methods by considering not only the state corresponding to the global minimum of the Gibbs function, but also other states occurring in case of the phase transformation.

A particle is considered as a closed thermodynamic system consisting of two limited mutually soluble components „1“ and „2“. When the solution is demixed, both components are redistributed between the two phases. The inclusion of a new phase is considered to be single in case of a small volume (demixing usually results in the occurrence of numerous inclusions in a macrosystem). The solutions formed in case of demixing wet each other, which contributes to the formation of core-shell structures [28]. The phase touching the boundaries of the system is further indicated by the index „s“ (shell), the phase in the center of the particle is indicated by the index „c“ (core). The conditions for the preservation of the substance are determined by the initial composition of the system

$$n_1 = n_{1c} + n_{1s}, \quad n_2 = n_{2c} + n_{2s},$$
$$x = \frac{n_2}{n_1 + n_2}, \; x_{ic} = \frac{n_{ic}}{n_{1c} + n_{2c}}, \; x_{is} = \frac{n_{is}}{n_{1s} + n_{2s}},$$

where n_i $(i = 1, 2)$ is the number of moles of components in the system, n_{ij} $(j = s, c)$ is number of moles in coexisting phases, x and x_{ij} are the molar fractions of components in the system and individual phases.

The sizes and surface area of spherical particles are determined by the composition of n_1, n_2 system and the molar volumes of the components V_1, V_2.

$$v_0 = n_1 V_1 + n_2 V_2, \quad r_0 = \sqrt[3]{\frac{3}{4\pi} v_0}, \quad A_0 = 4\pi r_0^2,$$

where v_0, r_0 and A_0 are the volume, radius, and area of the outer boundary of the system. The volume v_c, the radius r_c and the area of the interphase boundary A_{cs} with a spherical shape of the phase are determined by its composition n_{1c}, n_{2c}

$$v_c = n_{1c} V_1 + n_{2c} V_2, \quad r_c = \sqrt[3]{\frac{3}{4\pi} v_c}, \quad A_{cs} = 4\pi r_c^2.$$

Taking into account the surface energy of the interfaces, the Gibbs function of an individual particle has the form

$$g = n_{1c}\mu_{1c} + n_{1s}\mu_{1s} + n_{2c}\mu_{2c} + n_{2s}\mu_{2s} + \sigma_0 A_0 + \sigma_{cs} A_{cs}, \tag{1}$$

where $\mu_{ij} = \mu_{ij}^0 + RT \ln\left(\gamma_i(x_{ij}) x_{ij}\right)$ — chemical potential, σ_0, σ_{cs} — surface energy at the system surface and interface, $\gamma_i(x_{ij})$ — molar fractions and activity coefficients of components in the corresponding phases.

The reference values of the molar volumes and surface energy of the components and the equation of state of the solution [30] were used for numerical simulation of Bi–Sb mixture [29]. The approximation $\sigma(x) = \sigma_1 + x(\sigma_2 - \sigma_1)$ was used to calculate the surface energy of the solution [31]. If necessary, it can be replaced by well-known empirical and semi-empirical equations [32–34].

The parameters of the model are the quantities of components n_1, n_2 and the function (1) has two independent variables n_{1c} and n_{2c}. They can be replaced by normalized values $\theta_1 = n_{1c}/n_1$ and $\theta_1 = n_{1c}/n_2$, corresponding to the proportion of components that have entered the core phase [35]. The energy of the particle $g(\theta_1, \theta_2)$ is recalculated per mole of the mixture

$$G^E(\theta_1, \theta_2) = \frac{g(n_1, n_2, \theta_1, \theta_2) - g(n_1, n_2, 0, 0)}{n_1 + n_2}.$$

The surplus Gibbs energy relative to the homogeneous state makes it possible to compare the states of systems of any size, composition, and configuration (core-shell, janus or another [17]) in the form of a surface of surplus Gibbs energy $G^E(\theta_1, \theta_2)$, which in θ coordinates is expressed per single square. The results in numerical modeling are represented by a matrix of function values $G^E(\theta_1, \theta_2)$ on a grid with a step of $\Delta\theta$, which determines the accuracy of the calculation and the size of the matrix.

Let us consider the possibilities of θ-mapping by using the example of a segregating mixture of Bi–Sb, the size effects of which were modeled in Ref. [36,37]. The figure shows a characteristic view of the energy surface of the states of a segregating solution for particles of different sizes and compositions.

Special points correspond to thermodynamically equilibrium states in the diagram

$$\frac{\partial^2 G^E}{\partial\theta_1 \partial\theta_2} = 0.$$

The minima correspond to steady stable and metastable equilibria. The homogeneous state $G^E(0, 0)$ becomes stable under the condition

$$\frac{\partial G^E}{\partial\theta_1} \geq 0, \quad \frac{\partial G^E}{\partial\theta_2} \geq 0 \quad \text{(fig. } d\text{–}i\text{)}.$$

Bi–Sb mixture has two thermodynamically equilibrium heterogeneous states core@shell Bi@Sb and Sb@Bi, differing by the arrangement of coexisting phases [36]. Their position on θ-diagrams depends on the concentration of x and the volume of the system. They also demonstrate ravine trajectories corresponding to optimal paths between core–shell homogeneous and equilibrium states. They are defined by the conditions

$$\frac{\partial G^E}{\partial\theta_1} = 0, \quad \text{or} \quad \frac{\partial G^E}{\partial\theta_2} = 0$$

(numerically corresponds to the minimum values in the rows and columns of the matrix $G^E(\theta_1, \theta_2)$). The trajectories leading to the Sb@Bi state are shown in the figures with red lines and link the state of the homogeneous solution and the state in which Sb is concentrated in the core phase. The trajectories leading to the Bi@Sb state are shown by blue lines.

The inserts in the figure show the change of energy along ravine trajectories, the length of which is determined

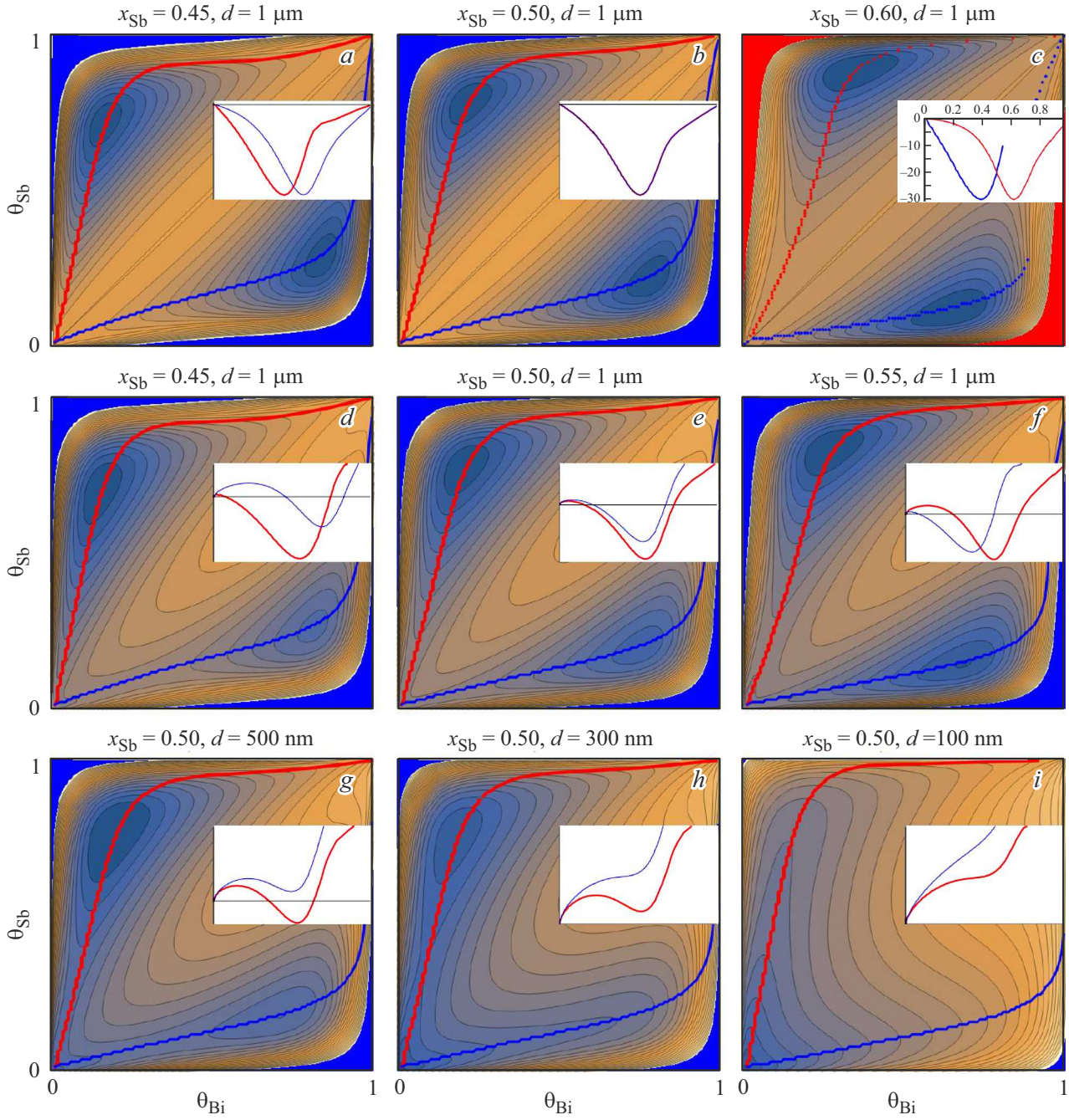

θ-diagrams of the particle state of Bi−Sb mixture depending on the diameter of particles (d) and concentration of Sb (x). The inserts demonstrate a change of the energy of the system along ravine trajectories.

by the total fraction of the substance that passed into the core phase ($\theta = (\theta_1 + \theta_2)/2$). The maxima on the curves correspond to the saddle points of θ-diagram, they coincide with unstable thermodynamic equilibria and the height of potential barriers.

The homogeneous state is thermodynamically unstable

$$\frac{\partial G^E}{\partial \theta_1} < 0$$

for macrosystem and large particles. It can spontaneously pass into any of the heterogeneous states (spinodal decay) with infinitely small fluctuations of composition (see inserts in figure a–c). Both core-shell states have equal energy and a composition of coexisting phases as long as the contribution of surface energy to $G^E(\theta_1, \theta_2)$ is negligible.

The proportion of surface energy increases by $G^E(\theta_1, \theta_2)$ with the decrease of the particle volume. This leads to a potential barrier that makes the homogeneous state stable and the core-shell states distinguishable (see Figure d–i). Since the core phase has a smaller boundary area, the transfer of a component with high surface tension (Sb) into

it is favorable in case of minimization of energy, as it puts the system in the Sb@Bi state (see Figure $d-i$).

The occurrence of the energy barrier changes the phase separation mechanism from spinodal (in the macrosystem) to binodal, with the formation of a new phase nucleus of critical size (critical nucleus) [38]. This can be seen when comparing θ-diagrams for particles with a diameter of 1 mm (Figure $a-c$) and 1 μm (Figure $d-f$). The height of the energy barriers significantly depends on the concentration and increases with the decrease of the volume. Heterogeneous states lose stability for nanoscale particles, and the homogeneous state remains the only equilibrium state (Figure $g-i$).

The saddle points on the θ-diagram can be homologated with the critical nuclei [39,40]. Two critical nuclei of different volume and composition occur in the considered system. Their growth puts the system in an equilibrium state. The composition of the nuclei changes with the growth, deviating from the equilibrium composition of the core phase by $\pm 1-2\%$. The possibility of the existence of more than two different critical nuclei follows from the results of Ref. [35].

It should be noted that the choice of the transformation path depends not only on the energy of the final equilibrium state. The probability and speed of the transition are affected by the size and energy of the formation of critical nuclei. The rate constants of many physical and chemical processes contain an Arrhenius multiplier $\exp(-\Delta G/RT)$, where the energy of formation of a critical nucleus determines the activation energy ΔG, T is the temperature, R is the gas constant. The size of the nucleus is hidden in the Arrhenius multiplier in the form of an enthalpy contribution, and it determines the effective cross-section of interaction with diffusing atoms in the pre-exponential multiplier. Thus, the formation of metastable Bi@Sb states may be more likely from the point of view of kinetics. A similar situation is typical for micron and submicron diameter particles with a high concentration of Sb (Figure f). An interesting effect is the reduction or complete absence of the spinodal decay region in small volume systems. The difficulty of nucleation in a small volume is discussed using a similar thermodynamic approach [41].

Taking into account the kinetic aspects, the θ-representation allows considering a particle with a segregating solution as a rather complex dynamic system and significantly complements $T-x$ and $P-x$ diagrams displaying only equilibrium states.

3. Conclusion

The construction of θ-diagrams is a convenient tool for assessing the thermodynamic stability of structures arising from phase transformations in a small volume and the ways of their formation. θ-diagrams demonstrate the emergence and evolution of stable and metastable states depending on the volume and composition of the system. These patterns are thermodynamic in nature and can be transferred to the behavior of similar objects of different chemical nature and composition. However, it should be noted that empirical and semi-empirical equations of state for real solutions that adequately describe characteristic curves (binodes, spinodes) and critical points do not guarantee the same accuracy when describing intermediate states in a two-phase or homogeneous region. Similar observations are valid for surface energy estimates. The related distortions of θ-diagrams do not change the positions of the singular points representing stable equilibrium states and defining the topology of the energy surface.

θ-diagrams make it possible to predict the reaction of a system to changes in its size and composition, to determine thermodynamically stable and metastable equilibrium states, and their stability. The analysis of the energy profile of the most probable paths of phase transformations makes it possible to evaluate the properties of critical nuclei and the probability of formation of different equilibrium states.

The visibility of θ-diagrams helps to understand the nature and behavior of such materials in their production, storage and operation conditions.

Funding

This study was carried out under the state assignment of the Razuvaev Institute of Organometallic Chemistry, Russian Academy of Sciences.

Conflict of interest

The author declares that he has no conflict of interest.

References

[1] K.R. Wilson, A.M. Prophet. Annu. Rev. Phys. Chem. **75**, *1*, 1 (2024).
[2] Z. Wei, Y. Li, R.G. Cooks, X. Yan. Annu. Rev. Phys. Chem. **71**, 31 (2020).
[3] J. Bauermann, S. Laha, P.M. McCall, F. JÜlicher, C.A. Weber. J. Am. Chem. Soc. **144**, *42*, 19294 (2022).
[4] V.B. Fedoseev, E.N. Fedoseeva. Kinet. Catal. **65**, *2*, 85 (2024).
[5] V.B. Fedoseev, T.A. Kovylina, E.N. Fedoseeva. Polym. Sci. Ser. B **66**, 138 (2024).
[6] V.B. Fedoseev. Tech. Phys. Lett. **49**, *4*, 71 (2023).
[7] R. Mendoza-Pérez, G. Guisbiers. Nanotechnology. **30**, *30*, 305702 (2019).
[8] F.H. Kaatz, A. Bultheel. Nanotechnology **29**, *34*, 345701 (2018).
[9] K.K. Bajpai, S.K. Shukla, S. Bhanu, S. Kankane. Prog. Polym. Sci. **33**, *11*, 1088 (2008).
[10] V. Marturano, P. Cerruti, M. Giamberini, B. Tylkowski, V. Ambrogi. Polymers. **9**, *12*, 8 (2016).
[11] H. Liu, X. Wang, D. Wu. Sustain. Energ. Fuels **3**, *5*, 1091 (2019).
[12] X. Wei, F. Xue, X.D. Qi, J.H. Yang, Z.W. Zhou, Y.P. Yuan, Y. Wang. Appl. Energy. **236**, *3*, 70 (2019).
[13] F. Wang, W. Lin, Z. Ling, X. Fang. Sol. Energy Mater. Sol. Cells **191**, *2*, 218 (2019).

[14] M.B. Gawande, A. Goswami, T. Asefa, H. Guo, A.V. Biradar, D.-L. Peng, R. Zboril, R.S. Varma. Chem. Soc. Rev. **44**, *21*, 7540 (2015).
[15] T. Philippe. Phys. Rev. E. **96**, *3*, 1 (2017).
[16] V.B. Fedoseev, E.N. Fedoseeva. Russ. J. Phys. Chem. A. **88**, *3*, 436 (2014).
[17] V.B. Fedoseev, A. V. Shishulin. Phys. Solid State **60**, *7*, 1398 (2018).
[18] V.M. Samsonov, I.V. Talyzin, A.Y. Kartoshkin, S.A. Vasilyev, M.I. Alymov. Comput. Mater. Sci. **199**, *7*, 110710 (2021).
[19] M. Ghasemi, Z. Zanolli, M. Stankovski, J. Johansson. Nanoscale **7**, *41*, 17387 (2015).
[20] V.M. Samsonov, A.Y. Kartoshkin, I.V. Talyzin, S.A. Vasilyev, I.A. Kaplunov. J. Phys. Conf. Ser. **1658**, *1*, 1 (2020).
[21] S. Bajaj, M.G. Haverty, R. Arróyave, W.A. Goddard Iii Frsc, S. Shankar, W.A. Goddard, S. Shankar. Nanoscale. **7**, *21*, 9868 (2015).
[22] G. Kaptay. J. Mater. Sci. **47**, *24*, 8320 (2012).
[23] D. Gross. Microcanonical thermodynamics: phase transitions in „small" systems. World Scientific. 66, (2001).
[24] E. Ma. Prog. Mater. Sci. **50**, *4*, 413 (2005).
[25] Z. Swiatkowska-Warkocka. Appl. Sci. **11**, *5*, 1978 (2021).
[26] S. Bogdanov, V. Samsonov, N. Sdobnyakov, V. Myasnichenko, I. Talyzin, K. Savina, V. Romanovski, A. Kolosov. J. Mater. Sci. **57**, *28*, 13467 (2022).
[27] V.M. Samsonov, N.Y. Sdobnyakov, A.Y. Kolosov, S.S. Bogdanov, I.V. Talyzin, S.A. Vasilyev, K.G. Savina, V.V. Puytov, A.N. Bazulev. Colloid J. **86**, *1*, 109 (2024).
[28] I.K. Razumov. Phys. Solid State. **66**, *9*. 1407 (2024).
[29] A.P. Babichev, N.A. Babushkina, A.M. Bratkovsky, et al. Fizicheskiye velichiny: Spravochnik. Energoatomizdat, Moscow (1991). (in Russian).
[30] M.A. Bykov, G.F. Voronin, N.M. Mukhamedzhanova. Pryamye i obratnye zadachi khimicheskoy termodinamiki. Nauka, Novosibirsk. (1987). P. 30. (in Russian).
[31] D. Hourlier, P. Perrot. Mater. Sci. Forum **653**, *77* (2010).
[32] B. von Szyszkowski. Zeitschrift Für Phys. Chemie. **64U**, *1*, 385 (1908).
[33] H.S. Umarkhadzhiev, R.Kh. Dadashev, S.M. Umarkhadzhiev, D.Z. Elimkhanov. Russ. J. Phys. Chem. **96**, 648 (2022).
[34] A.A. Afashagov, M.A. Shebzukhova. A.A. Shebzukhov. Phys. Solid State **64**, 293 (2022).
[35] V.B. Fedoseev, A.V. Shishulin, E.K. Titaeva, E.N. Fedoseeva. Phys. Solid State. **58**, *10*, 2095 (2016).
[36] V.B. Fedoseev. Phys. Solid State. **57**, *3*, 599 (2015).
[37] A.V. Shishulin, V.B. Fedoseev, A.V. Shishulina. Tech. Phys. **64**, *4*, 512 (2019).
[38] V.P. Skripov, A.V. Skripov. Sov. Phys. Usp. **22**, 389 (1979).
[39] C.N. Nanev. Theory of Nucleation. In Handbook of Crystal Growth. Elsevier. **1**, 315 (2015).
[40] M.P. Anisimov. Russ. Chem. Rev., **72**, 591 (2003).
[41] N. Ziethen, J. Kirschbaum, D. Zwicker. Phys. Rev. Lett. **130**, 248201 (2023).

Translated by A.Akhtyamov